NASA's Orion Crew Module Seakeeping Simulation and Test Comparisons in Ocean Wave Environments

Abigail Lockard
College of Engineering and Computer Science
Florida Atlantic University
Dania Beach, FL, USA
alockard2017@fau.edu

Tannen VanZwieten
Langley Research Center
National Aeronautics and Space Administration
Hampton, VA, USA
tannen.vanzwieten@nasa.gov

Jennifer Mann
Applied Physics Lab
Johns Hopkins University
Laurel, MD, USA
jennifer.mann@jhuapl.edu

Michael Keenan
College of Engineering
Georgia Institute of Technology
Atlanta, Georgia, USA
mkeenan7@gatech.edu

Christian Behrend
Johnson Space Center
Jacobs Technology
Houston, TX, USA
christian.c.behrend@nasa.gov

Benjamin Connell
Applied Physical Sciences Corp.
General Dynamics
Groton, CT, USA
bconnell@aphysci.com

***Abstract*—The NASA Orion Crew Module (CM) post-landing seakeeping and uprighting capabilities are being evaluated across a variety of ocean wave conditions. This paper provides an overview of quarter-scale and full-scale test data and how the data compare with the CM seakeeping dynamic simulation results evaluated using Wave Energy Convertor Simulator (WEC-Sim). This includes a discussion of the status of the dynamic modeling effort, correlation of model inputs with the wave field from the test, and a comparison of the results against the physical test data with emphasis on the full-scale results. Analysis in the frequency domain showed similar response characteristics between the model and the test and shows energy peaks corresponding to both the natural response and the forced response due to the wave environment. Time domain comparisons showed that the linear WEC-Sim model underpredicted the amplitude of the pitch and roll motion of the Buoyancy Test Article (BTA), with improved matching for smaller, longer crested waves. An attempt was made to correlate the pitch/roll response to incident wave slope to account for a possible delay in the BTA's response. The results did not show a strong relationship in the response characteristics to incident wave slope, but better correlation was seen by comparing responses in the frequency domain. Evaluation of the simulation's ability to match test results aided in understanding the current fidelity of the CM model in WEC-Sim and identifying areas for model improvement.**

Keywords—seakeeping, numerical modeling and simulation, Wave Energy Convertor Simulator (WEC-Sim), NASA, Orion, Crew Module Uprighting System (CMUS), Artemis I, Artemis II

I. Introduction

NASA's Artemis Program plans to launch the Orion Crew Module (CM) aboard the Space Launch System (SLS) from the Kennedy Space Center in Florida**.** The Orion CM is designed for a parachute descent and water landing following reentry or during the unlikely scenario of a launch abort**.** Following its splashdown in the open ocean, the CM Uprighting System (CMUS) is designed to upright the CM if it lands in the inverted orientation, is pulled over by the parachute, or is overturned due to large, steep waves. The CMUS consists of five deployable 55-inch diameter uprighting bags that are attached to the CM using multiple tethers (see Figs. 1 and 2)**.** The CMUS must meet requirements for successful reorientation of the CM from an inverted position (see Fig. 3) and provide a seakeeping capability until crew recovery begins. The CMUS must withstand loads on structural softgoods under a variety of sea conditions and system failures. The CMUS team is using a combination of testing and analysis to characterize the dynamic response of the CM and its ability to upright after splashdown in the ocean. The CM seakeeping response in waves (the subject of this paper) has been measured using both quarter-scale and full-scale test articles**.** In 2008, testing was conducted by the Naval Surface Warfare Center Carderock Division (NSWCCD) at Aberdeen Proving Ground in Maryland by using the quarter-scale Water Egress and Survival Trainer (WEST) to obtain dynamic response data [1, 2]. Tests were conducted for both monochromatic and sea state waves**.**

Fig. 1. Orion CM with CMUS bags after uprighting testing.

Fig. 2. Top-down view of the Orion CM with CMUS bags.

A full-scale test article called the BTA was used for seakeeping tests in 2018 as part of NASA's Underway Recovery Test-7 (URT-7) in the Pacific Ocean. The BTA was designed with geometry and mass properties similar to those of the Orion CM for the Artemis I mission. The goal of this testing was to collect an in-situ time history of incident waves as well as the BTA's response to those waves. The tests conducted at sea during URT-7 were designed to collect wave data via a dedicated hand-deployable buoy and BTA motion data that would be sufficiently correlated to compare the incident wave with the time-domain BTA response. This allows the same incident wave to be used in the simulation for a direct comparison between simulated CM motion predictions and the BTA response (in addition to using statistical characterization of at-sea data). The data were post-processed using the wave correlation method described in [1], which resulted in incident sea surface elevations that are time-correlated with the BTA motions.

To analyze the seakeeping of the CM under a wide range of conditions, a dynamic simulation was developed using an open-source tool called WEC-Sim. The WEC-Sim framework itself was developed as a collaboration between the National Renewable Energy Laboratories (NREL) and Sandia National Laboratories and funded by the U.S. Department of Energy's Waterpower Technologies Office. A linear WEC-Sim seakeeping model was used for this analysis, although WEC-Sim itself has options to support inclusion of nonlinearities. The simulated heave, roll, and pitch responses were compared with IMU response from both the quarter-scale and full-scale model tests. In the case of the WEST test, the time series of the incident waves was not measured. Instead, the wave spectra were measured, and several different realizations of the surface elevations time series were generated for use as an input to WEC-Sim. For the URT-7 test, the time-correlated data from [1] were used in the present analysis as the input to drive the WEC-Sim model. For this paper, emphasis is placed on the comparisons between the model predictions and test results for the full-scale BTA.

This paper is organized as follows: Section II discusses CM seakeeping modeling using WEC-Sim. Section III provides an overview of CM seakeeping experiments that were conducted with a quarter-scale test article, the method for generating statistically similar waves for use in WEC-Sim, and a comparison of the model and test results. Section IV provides an overview of full-scale seakeeping tests with in-situ wave measurements conducted during URT-7 in the Pacific, analysis of test results, and comparison against WEC-Sim CM seakeeping results using a similar input. Concluding remarks are provided in Section V.

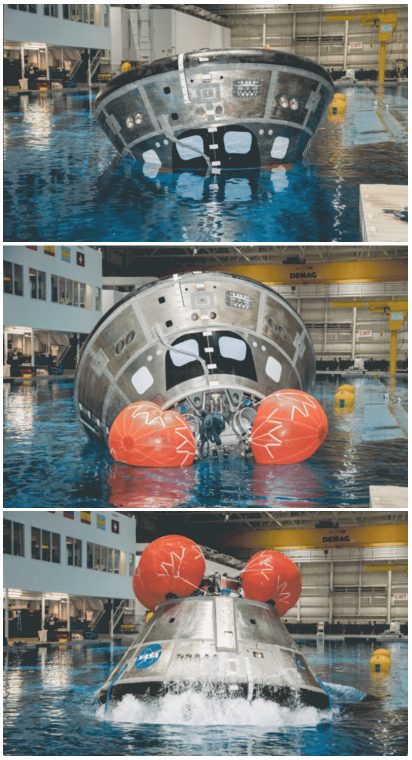

Fig. 3. CM uprighting tests conducted in the NASA NBL in 2017.

II. CM Simulation in WEC-Sim

The WEC-Sim is an open-source, MATLAB-based simulation tool designed to model wave energy converters (WECs) of various geometric characteristics operating in a wide range of environmental conditions. WEC-Sim is a multibody dynamics solver that uses Simscape Multibody in MATLAB and SIMULINK to solve for the dynamics of a system in wave environments [4]. WEC-Sim was designed to perform simulations of floating objects (wave energy converters or, in this case, the CM) by solving the governing equations of motion inclusive of user-provided hydrodynamic coefficients. These coefficients are developed using a frequency-domain boundary element method (BEM) solver to determine dynamics in the time domain (such as WAMIT, AQWA, NEMOH, and CAPYTAINE) [5, 6, 7]. The output files from these BEM solvers are used to calculate the various wave force components. WEC-Sim has the capability to model ocean systems in a wide variety of user-specified wave conditions, including predefined wave input options or user-defined waves. These simulations can be run using various wave input options.

For the Orion CM seakeeping analysis, model-specific parameters included the geometry, BEM data files that were generated using the NEMOH software (provided by Lockheed Martin (LM)), and quadratic damping coefficients that were determined through free-decay testing conducted in NASA's Neutral Buoyancy Laboratory (NBL). User-defined wave inputs

of time series of sea surface elevations were used to drive the simulation. These wave input files were specified such that they matched the as-tested wave conditions as closely as possible so that the modeled vehicle response could be compared with the response observed in testing to draw conclusions regarding the fidelity of the CM model in WEC-Sim. This analysis also provides information that can be used for future model fidelity improvements and scripts for conducting regression analysis.

III. Water Egress Survival Trainer (WEST) Tests

A. *WEST Test Overview*

Seakeeping experiments conducted with the WEST test article (quarter-scale model of the Orion CM) were completed under NASA's Constellation Program in 2008 [1, 2]. Tests were conducted for a range of mass properties, CM configurations (dry versus flooded, bare CM versus with stabilization collar, etc.), and wave conditions (monochromatic and sea states). The abort maximum mass, dry (i.e., no flooding), and bare (i.e., no collar) test setup was implemented in WEC-Sim for comparison against the WEST test results. These seakeeping tests were applied to aid in the evaluation of the response characteristics of the CM modeled in WEC-Sim. Static stability tests conducted for the WEST quarter-scale model were also leveraged to aid in understanding the regions under which a linear model of the CM is valid.

B. *WEST Static Stability Test*

The results of the nonlinear stability test conducted for the WEST test article are shown in Fig. 4, where GZ is the righting lever (highlighted in yellow) and GM is the metacentric height in inches. The nonlinear restoring force is proportional to GZ. The initial stability through the linear region is shown by the slope of the GZ curve at the origin. The behavior of the restoring force is linear up to approximately 5 degrees of rotation relative to the surface of the flat water, with the geometric nonlinearities becoming more significant beyond CM rotations of 10 degrees. By 26 degrees, the measured restoring force (Fig. 4, yellow curve) is at its maximum, and after this the stiffness gradient becomes negative. After 75 degrees, pitch restoring is lost in the absence of an uprighting system (stability bags).

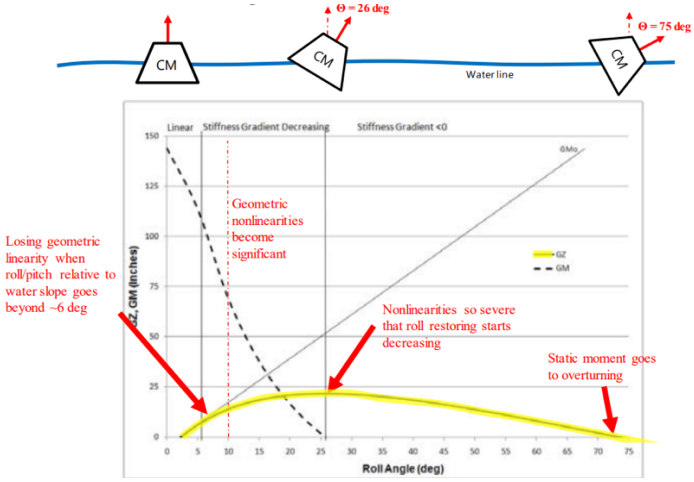

Fig. 4. Nonlinear stability test results for the quarter-scale WEST test article.

The Orion CM model developed using WEC-Sim at the time of this report uses a linear restoring force, such that the restoring forces increase linearly as the CM rotation angle increases. Thus, the simulated restoring forces begin to diverge significantly from the nonlinear restoring forces at CM rotation angles of approximately 10 degrees. This contributes to decreased model confidence as the dynamic motion of the CM increases in amplitude. Another contributor to lower model confidence for larger/steeper waves is the exclusion of surge motion. At lower sea states wave surfing is not a significant concern, but beyond SS4 the surge motion due to wave riding becomes prevalent in the WEST Test.

C. *Model Setup and Wave Input Generation for Time-Domain Sea State Comparisons*

To model the WEST test article in WEC-Sim, a scaled version of the CM with matching mass properties was evaluated against statistically similar wave inputs. The hydrodynamic coefficients for the quarter-scale model were provided by LM. The model fidelity was improved by including a quadratic damping coefficient that was tuned using free-decay data up to approximately 25 degrees of initial angular displacement. The linear model of the CM in WEC-Sim does not account for wave surge or wave riding (surfing) effects.

Wave inputs were generated based on the measured wave spectrum for each combination of sea state and CM configuration (note that multiple tests were conducted with the same target spectra and CM configuration, but only one wave spectrum measurement was documented). The spectrum does not define component wave phases, which are necessary for defining waves in the time domain. Thus, an inverse Fourier transform was implemented to generate time-domain wave profiles from the frequency data. By discretizing the wave spectra into regular wave components (see Fig. 5), time-domain wave profiles were generated by randomly changing the phase angle. This method was used to generate an hour of unique time-domain wave inputs for each sea state that were statistically similar to the waves generated for the tests. The wave inputs were divided into 3-minute samples to achieve durations in the range of WEST seakeeping test durations.

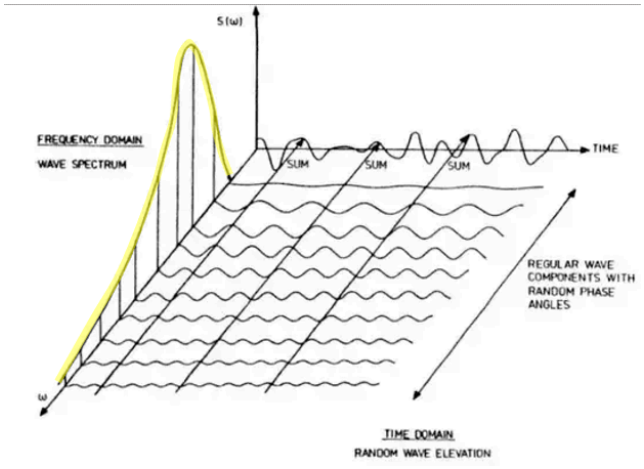

Fig. 5. Illustration of the connection between frequency-domain and time-domain representation of waves [5].

D. *Results from Time-Domain Sea State Comparisons*

The WEC-Sim CM seakeeping model was evaluated with and without the inclusion of pitch/roll quadratic damping and compared with the WEST results. Note that the choice of wave phases impacts the creation of wave groups and the largest wave amplitude observed in a given time frame. The maximum wave amplitude for a given spectrum is correlated to exposure time and probability of occurrence. This contributed to variations in the response characteristics between simulation and test. The inclusion of quadratic damping reduces the amplitude of rotation, with larger reductions as amplitude increases (since the damping is proportional to velocity squared). This led to decreased rotation angles in the simulation and results that were better correlated to those experienced during the WEST test for the maximum rotation. Table 1 provides maximum CM rotation angles for SS3 through SS6, revealing the reduction in peak angles observed in WEC-Sim (and improved matching) due to the inclusion of quadratic damping. For SS3 and SS4, a similar trend of improved matching with the inclusion of quadratic damping was observed when evaluating groups of the highest one-tenth and one-third of wave amplitudes peaks (not shown). Thus, the quadratic damping was included in the simulation to better capture peak responses of the CM, which will be a driver in performance and CMUS loads capability during station keeping and uprighting. The time domain response (not shown) demonstrated that the WEC-Sim model response did not exhibit the nonlinear behaviors observed in the WEST test article response (as expected for a linear model).

TABLE I. MAXIMUM CM ROTATION (DEGREE) FOR EACH SEA STATE

	WEC-Sim (no damping)	WEC-Sim (with damping)	WEST
SS3	14.7	13.1	13.0
SS4	27.0	21.3	23.4
SS5	35.9	30.3	32.7
SS6	53.7	42.9	27.7

Additional comparisons were conducted between WEC-Sim and the WEST test data for monochromatic waves with comparable wave slopes to the WEST SS5 and SS6 tests. The WEC-Sim model struggled to replicate WEST test results for these conditions (matching was not as close as for the sea state conditions primarily discussed here) and consistently underpredicted the maximum CM pitch/roll response (up to 88%). The lack of matching with the monochromatic waves where the target wave height and period are known for each test (making it easier to match wave inputs as compared with sea state data) contributes to decreased confidence as the wave height and steepness increases.

Additional challenges with the complete set of WEST test data include wavemaker limitations (the actual wave is not a reproduction of the desired wave), possible shallow water waves (wave breaking), and WEST test article rotating and drifting with unknown position and yaw angle. The results do provide confidence in the linear model with quadratic damping for lower sea states.

IV. URT-7 TESTS

A. *URT-7 Test Overview*

A series of URTs were conducted off the coast of Southern California through a collaborative effort between NASA's Exploration Ground Systems and Department of Defense personnel. URT-7 was the seventh in a series of tests designed to validate procedures and hardware that will be used to recover the CM after splashdown. This series of tests was conducted onboard the USS John P. Murtha, a San Antonio-class amphibious transport dock ship. During URT-7, a series of seakeeping tests were also conducted to support a secondary objective of collecting wave condition characteristics and CM response data for CMUS seakeeping analysis.

The concept of operations for the seakeeping tests involved specific runs outside the recovery operations during the 6 days of testing from October 30 to November 5, 2018. Seakeeping runs were conducted during a 30-minute testing window where the BTA was free drifting in the ocean. Instrumentation used during these tests included a Xsens MTiG-700 inertial measurement unit (IMU) onboard the BTA (providing the state vector of the CM test article) and a DWR-G4 wave buoy (providing in-situ wave measurements).

A predetermined acceptable distance between the wave buoy and the BTA aided in determining the deployment of the wave buoy relative to the BTA (see Fig. 6). The goal for each deployment was to minimize the number of redeployments needed while retaining sufficient correlation between the wave at the buoy location and a future/past wave at the BTA location. The BTA typically drifted faster than the wave buoy, requiring the wave buoy to be retrieved when it drifted outside the location of acceptable wave correlation and redeployed 50 m downwind of the BTA by a team of Navy personnel onboard a tender. As consistent with prior URTs that made use of this test article, it was observed that water leaked into the BTA. The exact quantity of water and motion sensitivity to seawater ingress was not evaluated.

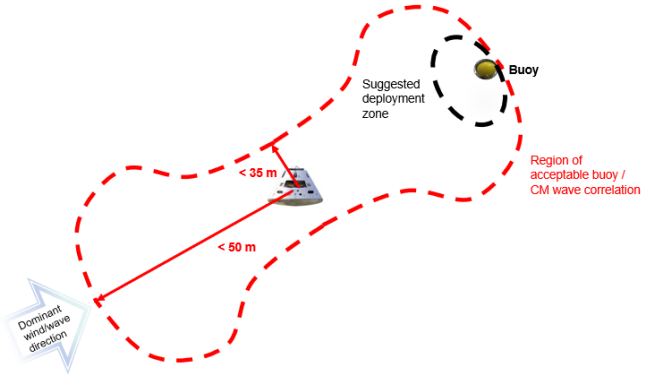

Fig. 6. Region of acceptable buoy and CM/BTA wave correlation used to guide buoy retrieval and re-deployment.

Using the wave correlation process described in [3], each of the wave buoy deployments (i.e., drift leg) was post-processed independently to estimate incident sea surface elevations at the location of the BTA. This was used as the WEC-Sim model input in the present analysis with the CM model adjusted to match the BTA's mass properties. The WEC-Sim model

response was then compared with the BTA test results for waves that were fully defined in the time domain. The full-scale nature of the test and knowledge of in-situ wave environments provided advantages over the statistical approach taken to evaluating the subscale results using the WEST data.

From the URT-7 tests, seven drift legs from two separate days at sea were post-processed to provide a side-by-side comparison of in-situ wave history and BTA IMU data. The actual drift of the buoy relative to the CM for each leg is presented in Figs. 7 and 8. Table II summarizes the wave conditions and BTA pitch and roll response for each leg. Significant wave height (SWH) was taken as an average of the top one-third of peaks throughout the leg. Wave period was taken as an average of the crest-to-crest time periods observed during the leg.

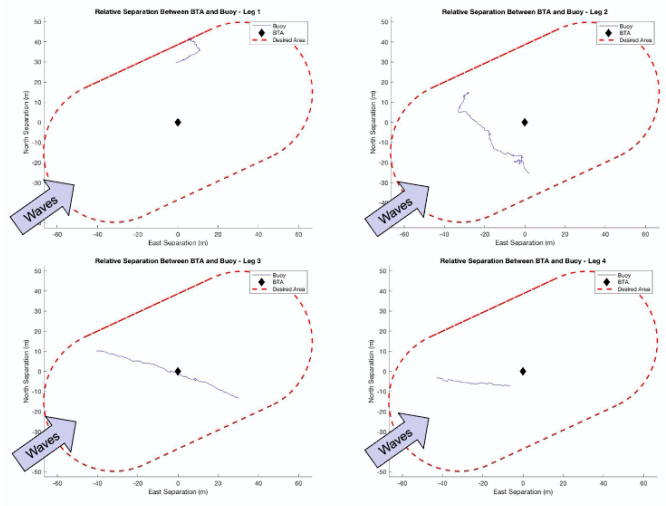

Fig. 7. Wave buoy position relative to the BTA for URT-7 10/31 test legs.

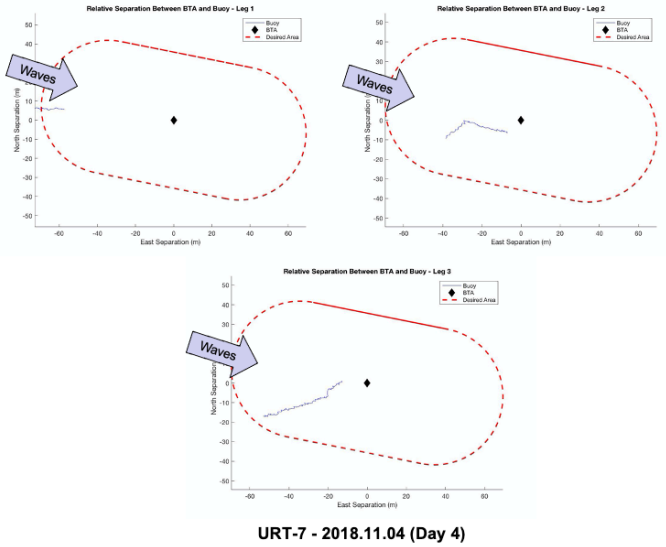

Fig. 8. Wave buoy position relative to the BTA for URT-7 11/04 tests legs.

TABLE II. CONDITION OVERVIEW OBSERVED DURING EACH LEG OF TESTING

URT-7 Test Leg	SWH (m)	Period (sec)	BTA RSS Max Response (deg)
10/31 Leg 1	0.998	10.414	4.926
Leg 2	0.847	10.517	6.763
Leg 3	0.783	8.813	6.376
Leg 4	0.892	5.945	4.833
11/04 Leg 1	1.062	8.891	10.972
Leg 2	1.511	8.503	9.015
Leg 3	1.364	9.709	11.5471

Fig. 9 provides a visual of various seakeeping tests conducted with respect to their SWH, mean wave period, and estimated mean wave slope for Orion landing zones. The wave slope statistics were calculated using the Bretschneider spectrum to estimate the most probable wave slope over a 2-minute time window. The URT-7 seakeeping test wave conditions were indicated on the chart based on the mean SWH and period from the wave buoy for each day of testing. The wave environments during both URT-7 seakeeping test days are within the region where linear CM response characteristics are anticipated (i.e., less than 10-degree CM rotation relative to the incident wave slope; figure with linear CM response estimates not shown). The wave environments from the WEST test (scaled to full scale) are also indicated in Fig. 9 to show the coverage of experimental data over the range of required landing conditions. Note that longer durations needed to meet the 24-hour seakeeping requirement would result in maximum wave slopes larger than shown.

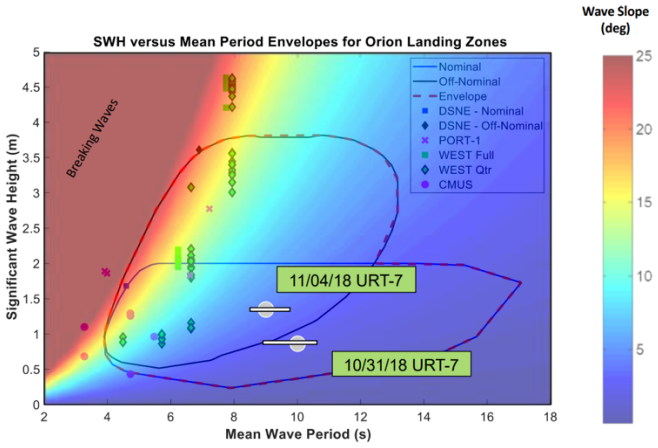

Fig. 9. URT-7 and WEST wave environments overlaid on plot of most probable maximum wave slope over a 2-minute exposure across range of SWHs and mean wave periods.

B. *Heave Results*

The time histories of the heave response for the WEC-Sim model and BTA provided for a given incident wave supplied a first look at their respective wave following characteristics before proceeding with the analysis of pitch and roll. Due to the variation in ability to correlate the buoy waves to the incident waves and wave profile characteristics, the BTA heave following of the buoy elevation varied from leg to leg (see Figs. 10 through 12).

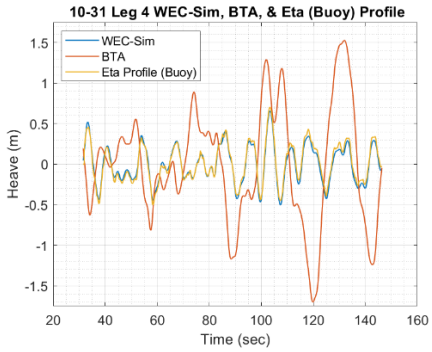

Fig. 10. 10/31 Leg 4 - Within region of acceptable wave correlation, matching results not satisfactory.

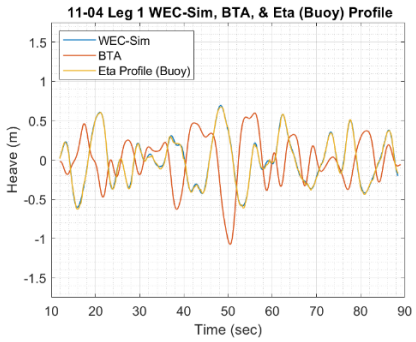

Fig. 11. 11/04 Leg 1 – Near perimeter of region of acceptable wave correlation, matching results remain satisfactory.

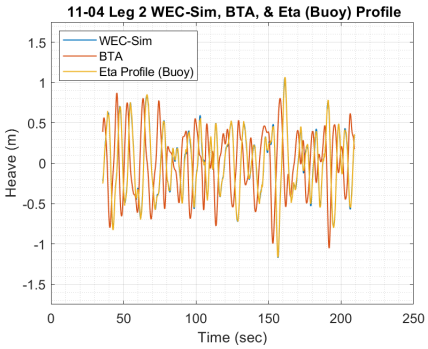

Fig. 12. 11/04 Leg 2 – Within region of acceptable wave correlation, matching results remain satisfactory.

Evaluation of the time series comparisons of the heave for the BTA, wave buoy, and CM in WEC-Sim provided in Figs. 10 through 12 and similar data from additional legs not shown led to a decision on which legs were sufficiently correlated to use for the pitch and roll analysis. The BTA heave does not track the eta profile for 10/31 Leg 4; therefore, this leg was not considered for the pitch/roll comparisons. Fig. 11 shows the maximum heave, as well as the mean of the top one-third heave responses for the wave buoy, BTA, and WEC-Sim results. The BTA response magnitudes for Leg 4 are out of family with their large magnitudes relative to the WEC-Sim heave and buoy elevations from other 10/31 legs. The remaining legs exhibited close wave following between the wave buoy and the WEC-Sim results and BTA heave motion. Therefore, the remaining legs were used for the pitch and roll analysis. The reason for the lack of wave following for Leg 4 is unknown, but it was noted that while the drift pattern met the requirements, the CM and buoy exhibited the fastest relative drift during this test leg.

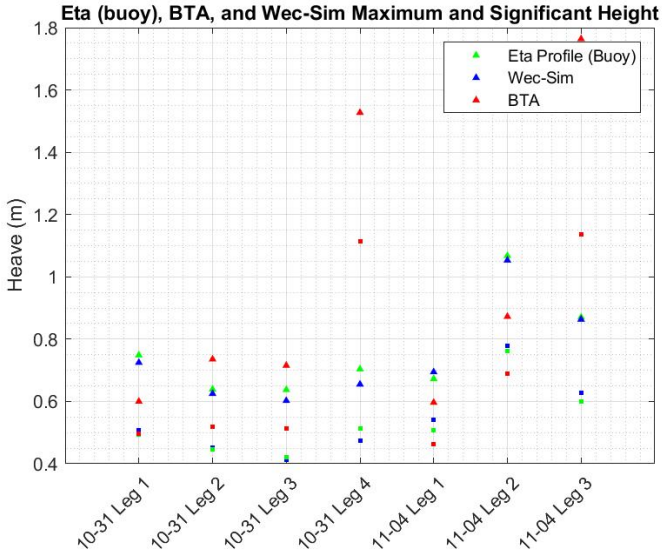

Fig. 13. Heave comparisons for model validation, where squares indicate the top one-third of responses and triangles indicate maximum heave response per leg.

For the heave motion statistics, the greatest difference in matching is seen in 10/31 Leg 4 and 11/04 Leg 3. The time domain results for 11/04 Leg 3 had satisfactory matching (results not shown) despite two large BTA heave peaks that skewed the peak and top one-third heave results appearing in Fig. 13. This contrasts with the 10/31 Leg 4 results, which were determined to be unsatisfactory due to the discrepancy of the wave buoy and BTA response data in the time domain. When comparing the BTA and WEC-Sim heave results, the BTA tends to exhibit more pronounced heave response characteristics and contains greater variation throughout the test legs.

C. Pitch and Heave Results

The root sum square (RSS) of pitch and roll was calculated to combine the rotational response of the system (i.e., eliminate the obscuring of the data due to variations in the yaw motion). The RSS was used for the analysis plots for both WEC-Sim and the BTA in Figs. 14 through 22. Fig. 14 shows a sample of the time domain comparison of the pitch and roll RSS of the BTA motion and WEC-Sim output. The comparisons across all legs are summarized in Fig. 15 with plots of the maximum and the mean of the top one-third RSSs of the angular response for the BTA and WEC-Sim. The WEC-Sim response underpredicts the BTA response for all included test legs (Fig. 15, summarized in Table II). Matching was better on the 10/31 test day, which had lower SWH and longer wave period conditions as compared with the 11/04 test day. Furthermore, the WEC-Sim predictions of the top one-third of the RSSs of the pitch/roll responses was better than the matching observed for the peak response measured for each leg (i.e., when results were averaged across several peaks).

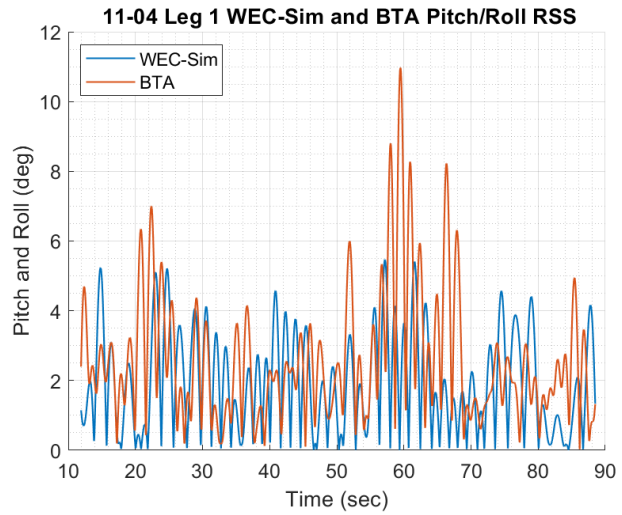

Fig. 14. RSS of BTA and WEC-Sim angular motions for 11/04 Leg 1.

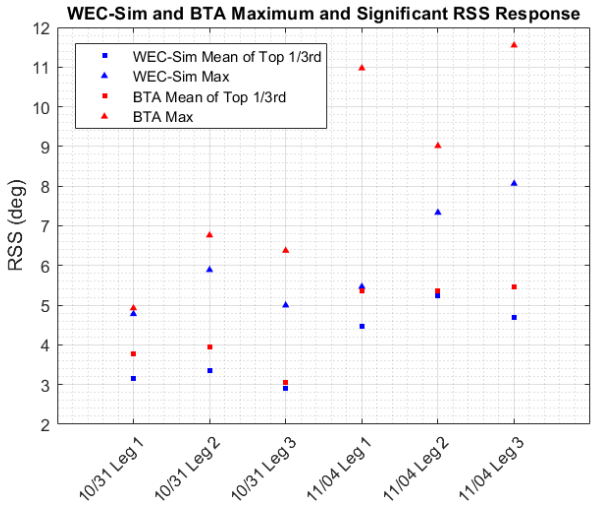

Fig. 15. Comparison of WEC-Sim and BTA response (Maximum and top one-third).

TABLE III. TIME DOMAIN ANALYSIS PERCENT ERROR

	Max RSS Response Matching Error	Avg of Max RSS Response Matching Error	Avg of Mean of top One-third RSS Response Matching Error
10/31, Legs 1-3	22%	13%	11%
11/04, Legs 1-3	50%	33%	11%

D. Slope Comparison for Pitch and Roll Results

Since ocean waves in this analysis were not monochromatic, another way to compare the pitch and roll response between the BTA and WEC-Sim was to plot the response as a function of the incident wave slope. The slope of an individual wave is defined as:

$$wave\ slope = ka$$

where k is the wave number and a is the wave amplitude. The wave number for each wave is defined as $k = \omega^2/g$ where the angular frequency of the wave as a function of the wave period, T, is $\omega = 2\pi/T$ and $g = 9.81\ \frac{m}{s^2}$ is the gravitational constant [5]. The wave slope was found for individual waves by extracting the corresponding crest-to-trough and trough-to-crest wave amplitudes and time periods. This created two different wave slope data sets for each leg that was analyzed. Wave slopes for the URT-7 legs were found to be small (less than 4 degrees) due to the combination of large wavelengths and relatively small wave amplitudes encountered during testing. Wave conditions on 11/04 had slightly steeper wave slopes than those observed on 10/31.

A comparison of pitch and roll RSS results was made with respect to wave slope in the time domain by looking at the RSS results from either crest-to-trough or trough-to-crest time windows. The results, shown in Fig. 16, did not show the expected increasing RSS response of the CM with an increase in wave slope. Instead, the measured CM RSS response showed a similar range of values across the 0- to 4-degree slope range. This may have been due to memory in the system, where the CM not only responded to the current incident wave but retained motion from previous incident waves.

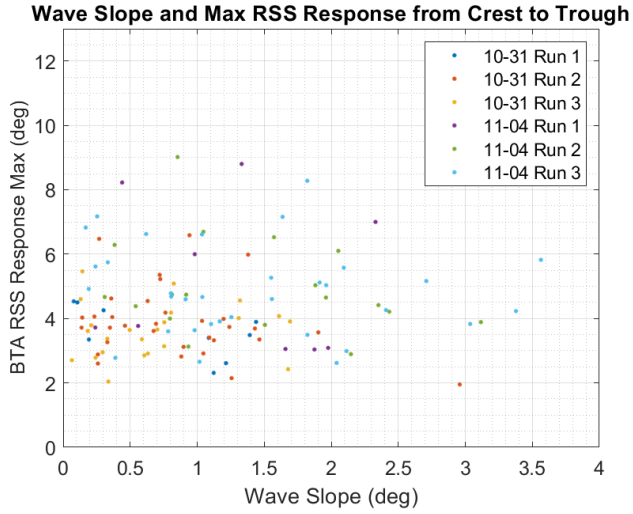

Fig. 16. Comparison of maximum pitch/roll RSS responses as a function of wave slope.

Having established this flat trend in pitch/roll response amplitude across the set of BTA results, the BTA pitch and roll responses were compared with the WEC-Sim results to check for matching. Figs. 17 and 18 show the mean and maximum (respectively) RSS responses from crest-to-trough as a function of wave slope for 10/31, Leg 2. WEC-Sim shows a similarly flat trend with large scatter in the CM response as was observed in the test data for both the mean and maximum values. As was observed previously with the heave response, WEC-Sim underpredicts the CM responses in pitch and roll.

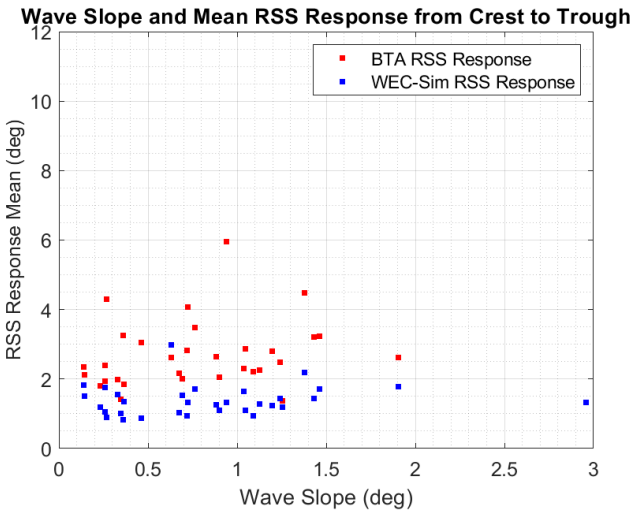

Fig. 17. Mean RSS response of pitch and roll with respect to crest-to-trough wave slope for 10/31 Leg 2.

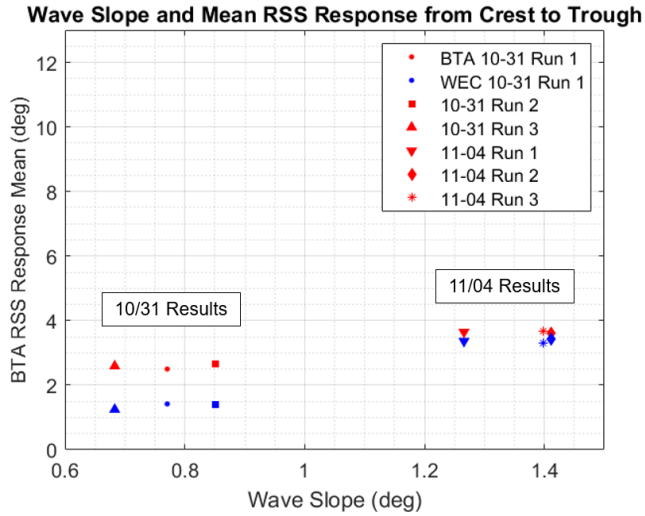

Fig. 19. Mean of the RSS pitch/roll mean responses and as a function of the mean wave slope for each leg.

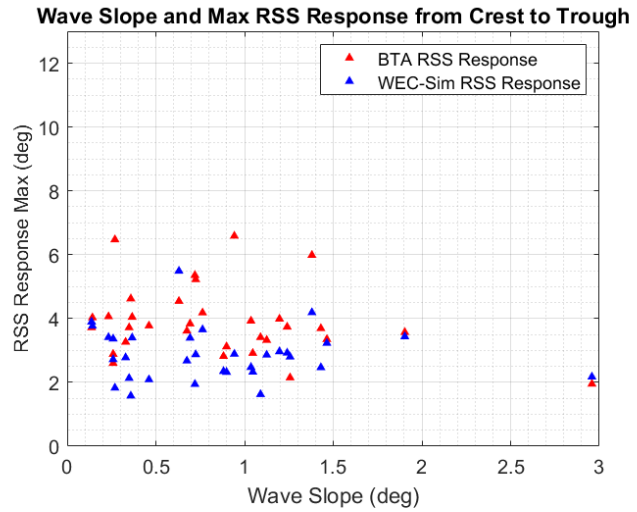

Fig. 18. Max RSS response of pitch and roll with respect to crest-to-trough wave slope for 10/31 Leg 2.

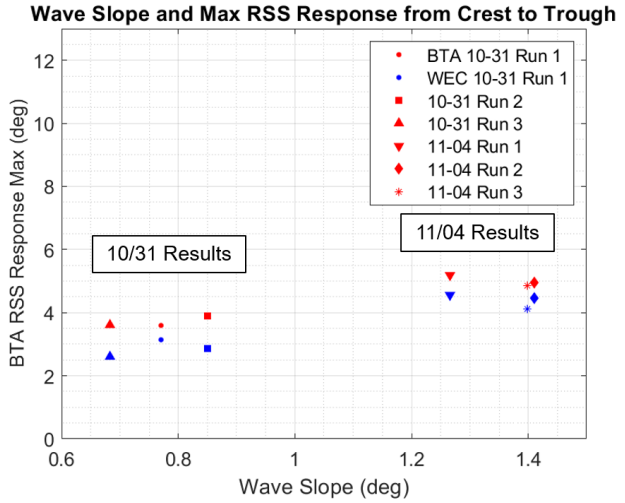

Fig. 20. Mean of the max RSS pitch/roll response as a function of mean wave slope for each leg.

To compare the mean and maximum responses across the available sets of data, the mean and maximum RSS responses (examples of which are provided in Figs. 17 and 18) were averaged across each leg for the BTA and corresponding WEC-Sim runs, and the resulting data is provided in Figs. 19 and 20. The average of the mean and max of the responses from WEC-Sim match the BTA responses to within one degree, with WEC-Sim consistently underpredicting the response for a given mean wave slope. These results also show better matching on the 11/04 test date, which had larger wave slope and pitch/roll responses.

A hypothesis for the lack of correlation between the wave slope and the BTA/WEC-Sim model response was the delay between the incident wave and the response. Thus, lagging peak responses were captured for a time segment larger than the crest-to-trough or trough-to-crest incident wave half-period that was used to determine the wave slope. A sample of this windowing strategy is shown in Fig. 21, where the large RSS spike observed after the crest-to-trough period is captured with the larger window.

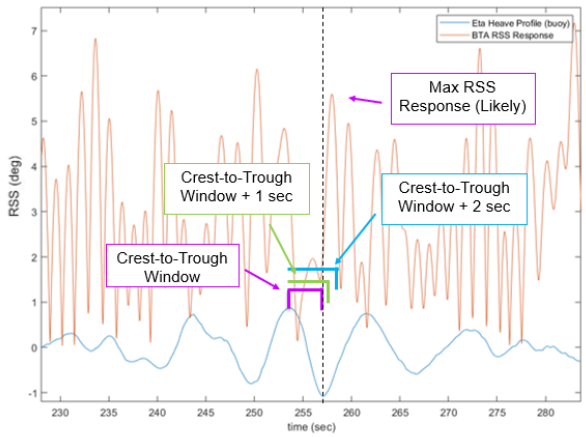

Fig. 21. Windowing strategy used to analyze RSS peak responses beyond the crest-to-trough half-period used to evaluate the incident wave slope.

A sample of the windowing results from 11/04, Leg 2 is shown in Fig. 22. WEC-Sim results were compared across ranges that included the crest-to-trough window plus 1, 2, and 3 seconds to capture a range of possible time shifts in the maximum response. Despite the windowing strategy, the flat trend across the leg remained consistent with the original analysis, and the WEC-Sim model response characteristics were not significantly altered.

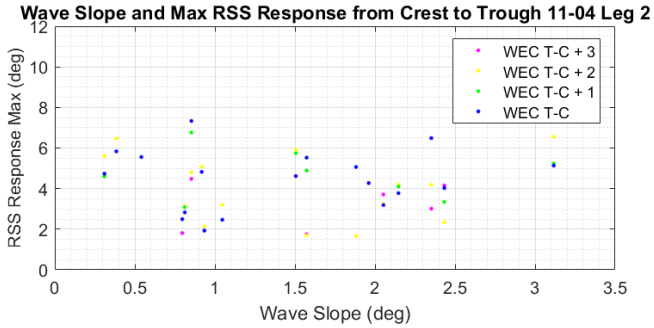

Fig. 22. Windowing results for crest-to-trough found by increasing the RSS pitch/roll response window for time periods 1, 2, and 3 seconds longer than the original time period.

E. Frequency Domain Results

Power spectral density (PSD) plots of the RSS pitch and roll response were calculated to provide comparisons across the entire response environment for both the WEC-Sim model and the BTA results. PSD plots of the pitch and roll RSS for both WEC-Sim and BTA responses are shown in Fig. 24. Each leg of the test day was co-plotted to compare the frequency characteristics of the unique wave environments. Two energy peaks are observed in this analysis: (1) the forced response near the peak incident wave frequency shown in Fig. 23 and (2) the natural response, which appears at higher frequencies (approximately the natural frequency of the system). For (1), the response of the BTA and WEC-Sim have a similar energy peak at the period corresponding to the dominant wave energy (around 10 seconds). Due to variations in the dominant wave energy from leg to leg, there is variation seen in individual leg PSDs. This variation between legs is expected because of the short duration of each leg. For (2), WEC-Sim consistently captures the BTA's natural frequency response around 3 seconds.

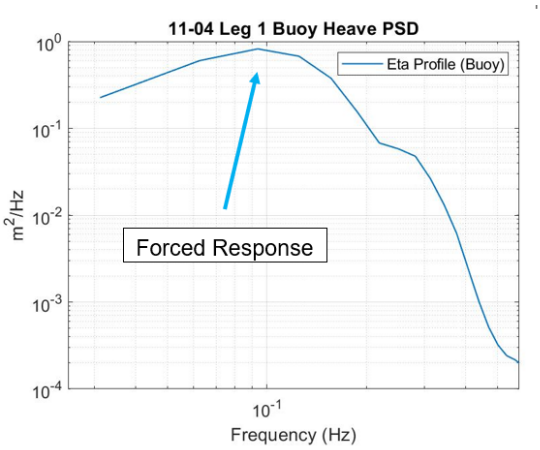

Fig. 23. PSD plot for 11/04 Leg 1 DWR wave buoy heave motion, which indicates the frequency of the forced response or dominant wave energy impacting the BTA.

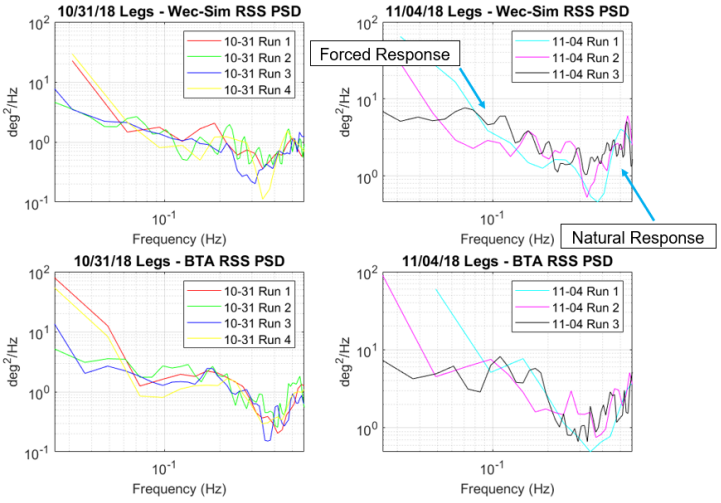

Fig. 24. 10/31 and 11/04 BTA and WEC-Sim pitch and roll RSS PSD plots for test leg.

To compare across all legs, the PSDs for each day were averaged to provide a general view of how well-matched the WEC-Sim model is to the BTA response (see Fig. 25). These PSD charts average the time-dependent events in favor of emphasizing the average response experienced by the BTA and the WEC-Sim model. The side-by-side comparison of the WEC-Sim and BTA results shown in Fig. 25 reveals that slightly less energy was observed from the WEC-Sim results for the 10/31 test day (consistent with time-domain observations). The 11/04 test day shows very close matching in the frequency domain in both the forced response and natural response regions. The comparison of the mean responses across the legs occurring each day (BTA versus WEC-Sim model) more clearly shows matching of the tilt response for the dominant wave energy for that day and natural response characteristics.

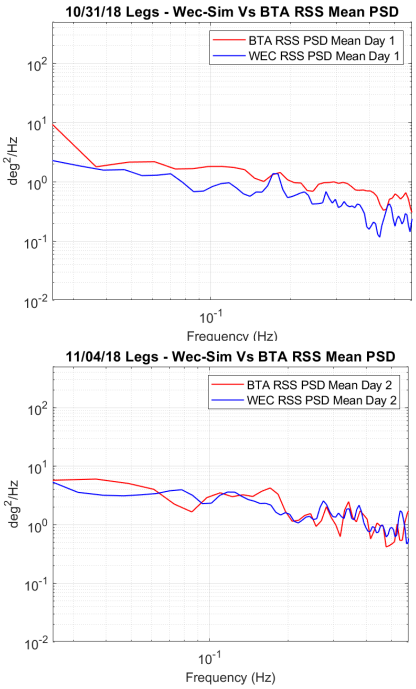

Fig. 25. 10/31 and 11/04 BTA and WEC-Sim pitch and roll RSS PSD plots, where all test legs from each day were averaged to yield a clear comparison for the energy matching between WEC-Sim and the BTA response.

Analysis from the frequency domain comparisons also supplies a possible explanation for the lack of correlation between wave slope and the RSS of the pitch/roll response discussed previously (shown in Figs. 17 through 20). In the wave environments observed during URT-7, the CM response is dominated by energy in the resonant band with a second energy peak corresponding to the wave field at a higher frequency (refer to Figs. 23 and 24). The CM response as a function of wave slope is therefore obscured by the resonant response of the CM, leading to low correlation between wave slope and the response of the CM.

V. Conclusions

The CM model/test comparisons discussed in this paper provide insight into the performance of the WEC-Sim model across a range of environments. Analysis was provided in this paper to compare the linear seakeeping simulation of the CM built in WEC-Sim with results from two different test campaigns: (1) quarter-scale WEST tests conducted in a range of sea state environments and (2) full-scale testing during URT-7 with more benign sea conditions and in-situ wave measurements in the Pacific Ocean. The WEC-Sim model consisted of a mostly linear model with the inclusion of quadratic damping to improve matching with WEST sea state data.

Challenges with the WEST test data included wavemaker limitations (actual wave is not a reproduction of the desired wave), WEST test article rotating and drifting with unknown position and yaw angle, use of a subscale model, and wave breaking/surfing, which was not captured in the WEC-Sim model. Results showed that the WEC-Sim model results did not exhibit the nonlinear behavior observed in the WEST test article response (as expected for a linear model), and it underpredicted the maximum peaks observed in the WEST test. Results from the URT-7 tests showed that the WEC-Sim model has the largest error in modeling the maximum peaks, but the correlation with measured response data improves significantly as the data are averaged across more data peaks. Overall, WEC-Sim produced a better match for more benign sea conditions and was challenged in matching the peaks of steep, large-amplitude waves. Additional model development would be useful to accurately predict the CM response in higher sea states.

Acknowledgment

The authors gratefully acknowledge the CMUS Team members from NASA's Johnson Space Center, the NESC, and LM for their work in developing the WEC-Sim simulation, conducting seakeeping tests, and providing the data needed to support the analysis. This includes Tara Angstadt, Molly Selig, James Dearman, Bill Milewski, Nathan Tom, and Ivan Bertaska. Funding for this work was provided by the NESC under assessment number TI-18-01308.

References

[1] T. Carrico, "Seakeeping Performance of NASA's Orion Crew Module," in *The 29th American Towing Tank Conference*, Annapolis, Maryland, 2010.

[2] T. Carrico, L. Hanyok and R. Banko, "Quarter Scale Orion Command Module Towing and Seakeeping Experiments," Naval Surface Warfare Center Carderock Division, West Bethesda, Maryland, 2009.

[3] I. R. Bertaska, T. VanZwieten, J. Mann, B. Connell, T. Radke and M. Bernatovich, "Dynamic Characterization of the Crew Module Uprighting System for NASA's Orion Crew Module," in *OCEANS 2019*, Seattle, WA, 2019.

[4] National Renewable Energy Laboratory and National Technology and Engineering Solutions of Sandia, LLC, "WEC-Sim v4.2 Theory," 2021. [Online]. Available: https://wec-sim.github.io/WEC-Sim/master/man/theory.html. [Accessed July 2021].

[5] C. H. Lee and J. N. Newman, "WAMIT User Manual, Version 7.4," WAMIT, Inc., Cambridge, MA, 2020.

[6] A. Babarit and G. Delhommeau, "Theoretical and numerical aspects of the open source bem solver nemoh," in *11th European Wave and Tidal Energy Conference (EWTEC2015)*, Nantes, France, 2015.

[7] ANSYS, Inc., "AQWA manual Release 15.0," Canonsburg, PA, 2013.

[8] O. M. Faltinsen, Sea Loads on Ships and Offshore Structures, Part of Cambridge Ocean Technology Series, Cambridge University Press, 1991.

[9] R. G. Dean and R. A. Dalrymple, Water Wave Mechanics for Engineers and Scientists, World Scientific, 1984.